Supporting Information (SI)

Pyridinylphosphorothioate-based blue iridium(III) complex with double chiral centers for circularly polarized electroluminescence

Jun-Jian Lu,[1,3#] Zhen-Long Tu,[1#] Xu-Feng Luo,[1] Yi-Pin Zhang,[1] Zhong-Ze Qu,[1] Xiao Liang,[1] Zheng-Guang Wu,[2*] You-Xuan Zheng[1*]

[1]State Key Laboratory of Coordination Chemistry, Jiangsu Key Laboratory of Advanced Organic Materials, School of Chemistry and Chemical Engineering, Nanjing University, Nanjing 210093, P. R. China. E-mail: yxzheng@nju.edu.cn.

[2]Nantong Key Lab of Intelligent and New Energy Materials, College of Chemistry and Chemical Engineering, Nantong University, Nantong, 226019, P. R. China. E-mail: wuzhengguang_zy@163.com.

[3]Hunan Provincial Key Laboratory of Fine Ceramics and Powder Materials, School of Materials and Environmental Engineering, Hunan University of Humanities, Science and Technology, Loudi, Hunan 417000, China. E-mail: lujunjian2001@126.com.

#Lu and Tu have same contribution to this paper.

Contents

S1. General information

^{1}H NMR spectra were measured on Bruker AM 400 spectrometer. The high resolution electrospray ionization mass spectra (HR ESI-MS) were recorded on an Bruker MTQ III q-TOF. Thermal analysis was measured on PerkinElmer Pyris 1 DSC under nitrogen at a heating rate of 10 ^oC min^{-1}. UV-vis absorption and photoluminescence spectra were measured on Shimadzu UV-3100 and Hitachi F-4600 spectrophotometer at room temperature, respectively. Cyclic voltammetry measurement was carried out using chi600 electrochemical workstation with Fc^+/Fc as the standard at the rate of 0.1 V s^{-1}, using CH_2Cl_2 and tetramethylammonium hexafluorophosphate as the solvent and electrolyte salt, respectively. The decay lifetime was measured with a HORIBA Scientific 3-D fluorescence spectrometer. The circular dichroism (CD) spectra were measured on a Jasco J-810 circular dichroism spectrometer with a scan speed of 200 nm/min with 1 nm resolution and a respond time of 1.0 s. The circularly polarized luminescence (CPL) and circularly polarized electroluminescence (CPEL) spectra were measured on a Jasco CPL-300 spectrophotometer based on 'Continuous' scanning mode at 200 nm/min scan speed. The test mode adopts "Slit" mode with the *E*x and *E*m Slit width 3000 μm and the digital integration time (D.I.T.) is 2.0 s with multiple accumulations (10 times or more).

X-ray crystallographic measurements of the single crystals were carried out on Bruker APEX-II CCD diffractometer (Bruker Daltonic Inc.) using monochromated Ga Kα radiation (λ = 0.71073 Å) at room temperature. Cell parameters were retrieved using SMART software and refined using SAINT[1] program in order to reduce the highly redundant data sets. Data were collected using a narrow-frame method with scan width of 0.30° in ω and an exposure time of 5 s per frame. Absorption corrections were applied using SADABS[2] supplied by Bruker. The structures were solved by direct methods and refined by full-matrix least-squares on F^2 using the program SHELXS-2014. The positions of metal atoms and their first coordination spheres were located from direct-Emaps, other non-hydrogen atoms were found in alternating difference Fourier syntheses and least-squares refinement cycles and during the final cycles refined anisotropically. Hydrogen atoms were placed in calculated position and refined as riding atoms with a uniform value of U_{iso}.

S2. Experiment section

The $[(dfppy)_2Ir(\mu\text{-}Cl)]_2$ chloride-bridged dimmer was prepared according to the reported method.

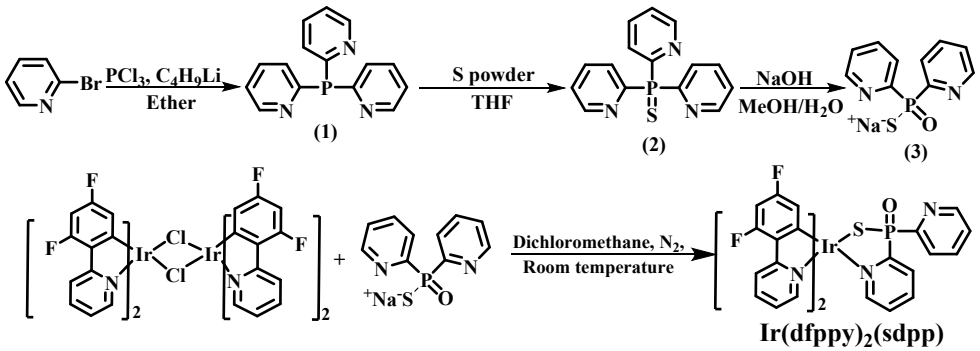

Scheme S1. Synthesis of the ancillary ligand and Ir(dfppy)$_2$(sdpp).

2.1 Synthetic Procedures

2.1.1 Tri(2-pyridine)phosphine (1)

A solution of 2.5 N *n*-butyllithium (6.40 mL, 16.00 mmol) in 15 mL of Et_2O was cooled to -78 ^oC, and 2-bromopyridine (2.52 g, 15.94 mmol) in Et_2O (6 mL) at -78 ^oC was added, and the dark red solution was stirred for 4 h at this temperature. A solution of phosphorus trichloride (0.74 g, 5.40 mmol) in Et_2O (10 mL) was added dropwise during 1 h at -78 ℃ and the solution was stirred at -78 ℃ for 2 h before warming slowly to room temperature. The tan-colored mixture was stopped with H_2SO_4 (20 mL, 2N) and the solution made alkaline with saturated NaOH solution to precipitate solid. The solid product was collected and recrystallized from acetone-petroleum (1:1, v/v) to get 0.59 g pure product with 41.09% yields.

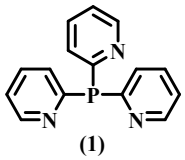

(1)

^{1}H NMR (400 MHz, $CDCl_3$) δ 8.65 (dt, J = 4.8, 1.4 Hz, 3H), 7.55 (tt, J = 7.7, 2.0 Hz, 3H), 7.34 (ddt, J = 7.8, 2.1, 1.1 Hz, 3H), 7.15 (ddt, J = 7.5, 4.8, 1.2 Hz, 3H). ^{31}P NMR (162 MHz, $CDCl_3$) δ -0.79 (s).

2.2.2 Sulfide-dipyridinylphosphinate (sdpp) (2)

The *tri*(2-pyridine)phosphine (0.59 g, 2.22 mmol) was then dissolved in tetrahydrofuran (30 mL) with S_8 (0.64 g, 2.5 mmol) and refluxed overnight under argon, giving the crude product sulfide-dipyridinylphosphinate. Then, the solvent was removed and the crude product was purified by column chromatography with CH_2Cl_2: petroleum ether = 2:1 as eluent with a yield of 75% (0.49 g).

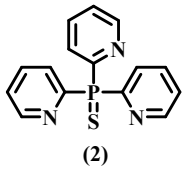

(2)

^{1}H NMR (400 MHz, $CDCl_3$) δ 8.80-8.74 (m, 3H), 8.31 (ddt, *J* = 7.8, 6.6, 1.1 Hz, 3H), 7.83 (tdd, *J* = 7.7, 4.5, 1.8 Hz, 3H), 7.38 (dddd, *J* = 7.7, 4.5, 2.9, 1.2 Hz, 3H). ^{31}P NMR (162 MHz, $CDCl_3$) δ 34.06 (s).

2.2.3 Sodium dipyridinylphosphorothioate (sdppNa) (3)

sdpp (0.49 g, 1.84 mmol) was dissolved in methanol (5 mL)/H_2O (5 mL), and the mixture was stirred at room temperature for 30 minutes. Sodium hydroxide (0.22 g, 5.55 mmol) aqueous solution was added, and the mixture was stirred at room temperature for 24 h. Then, the solvent was removed, and the residue was extracted with MeOH (15 mL), concentrated and dried to give the sodium dipyridinylphosphorothioate (0.72 g) with about 80% yields without further purification.

2.2.4 Ir(dfppy)$_2$(sdpp)

[(dfppy)$_2$Ir(μ-Cl)]$_2$ (1.15 g, 0.95 mmol) and 2.5 equivalent sdppNa (0.6 g, 2.37 mmol) were dissolved in 10 mL of dichloromethane. After degassed, the reaction was stirred at room temperature for about 10 min under argon. Then the solvent was removed and the crude compound was purified by column chromatography with $CHCl_3$:MeOH = 20:1 as eluent. Further purification was taken by gradient sublimation with a yield of 30.1% (0.45 g). Then, four chiral Ie(III) isomers were obtained by separation on the optical resolution of chiral high performance liquid chromatography (HPLC). The final products were fully characterized by ^{1}H NMR, ^{13}C NMR, high-resolution mass spectroscopy (HRMS) and single-crystal structure analyses.

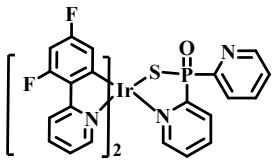

Ir(dfppy)$_2$(sdpp)

^{1}H NMR (400 MHz, $CDCl_3$) δ 9.92 (s, 1H), δ 8.21 (d, J = 8.3 Hz, 2H), 7.82-7.76 (m, 2H), 7.72-7.64 (m, 4H), 6.94 (ddd, *J* = 7.4, 5.9, 1.4 Hz, 2H), 6.69 (dd, *J* = 1.9, 0.6 Hz, 2H), 6.43 (ddd, *J* = 12.6, 9.2, 2.4 Hz, 3H), 6.14 (t, *J* = 2.0 Hz, 2H), 5.73 (dd, *J* = 8.6, 2.4 Hz, 2H). ^{19}F NMR (376 MHz, $CDCl_3$) δ −106.59 (1F), −108.49 (1F), −109.02 (1F), −110.64 (1F). ^{31}P NMR (162 MHz, Chloroform-d) δ 60.40, 61.05. HR ESI-MS (M/Z): Calcd for $C_{32}H_{20}F_4IrN_4OPS$ $[M+H]^+$: 809.0734, Found 809.0732.

λ-Ir(dfppy)$_2$(*S*-sdpp)

^{1}H NMR (400 MHz, $CDCl_3$) δ 8.74 (s, 1H), 8.47 (s, 1H), 8.27 (s, 1H), 8.21–8.14 (m, 1H), 8.07 (s, 1H), 7.97 (ddt, *J* = 7.5, 6.3, 1.2 Hz, 1H), 7.85 (s, 3H), 7.52 (s, 3H), 7.36 (s, 1H), 7.22 (d, J = 26.2 Hz, 2H), 6.55 (s, 2H), 6.35 (s, 1H), 5.56 (s, 2H). ^{19}F NMR (376 MHz,

Chloroform-d) δ -106.56 (1F), -107.69 (1F), -108.82 (1F), -110.58 (1F). ^{31}P NMR (162 MHz, Chloroform-d) δ 61.18.

δ-Ir(dfppy)$_2$(*R*-sdpp)

^{1}H NMR (400 MHz, $CDCl_3$) δ 8.48 (s, 1H), 8.20 (s, 3H), 7.86 (s, 1H), 7.74 (d, *J* = 38.3 Hz, 4H), 7.44 (s, 1H), 7.28 (s, 2H), 7.13–6.97 (m, 4H), 6.46 (s, 1H), 6.26 (s, 1H), 5.71 (s, 1H), 5.41 (s, 1H). ^{19}F NMR (376 MHz, Chloroform-d) δ -106.41(1F), -107.67 (1F), -108.98 (1F), -110.58 (1F). ^{31}P NMR (162 MHz, Chloroform-*d*) δ 61.24.

λ-Ir(dfppy)$_2$(*R*-sdpp)

^{1}H NMR (400 MHz, $CDCl_3$) δ 8.38 (s, 1H), 8.14 (d, *J* = 38.4 Hz, 2H), 7.98 (s, 1H), 7.89 (s, 1H), 7.73 (d, *J* = 31.1 Hz, 3H), 7.44 (s, 3H), 7.28 (s, 1H), 7.05 (d, *J* = 43.4 Hz, 3H), 6.45 (s, 2H), 6.27 (s, 1H), 5.49 (s, 2H). ^{19}F NMR (376 MHz, Chloroform-*d*) δ -106.55 (1F), -107.68 (1F), -108.79 (1F), -110.58 (1F). ^{31}P NMR (162 MHz, Chloroform-*d*) δ 62.11.

δ-Ir(dfppy)$_2$(*S*-sdpp)

^{1}H NMR (400 MHz, $CDCl_3$) δ 8.59 (s, 1H), 8.32 (d, *J* = 20.6 Hz, 2H), 7.97 (s, 1H), 7.89 (s, 2H), 7.80 (s, 2H), 7.55 (s, 2H), 7.38 (s, 1H), 7.12 (s, 3H), 6.55 (s, 1H), 6.35 (s, 1H), 5.79 (s, 1H), 5.62 (s, 1H), 5.52 (s, 1H), 4.97 (s, 1H). ^{19}F NMR (376 MHz, Chloroform-*d*) δ -106.59 (1F), -108.52 (1F), -109.05 (1F), -110.64 (1F). ^{31}P NMR (162 MHz, Chloroform-*d*) δ, 62.29.

2.2 NMR and HMMS spectra

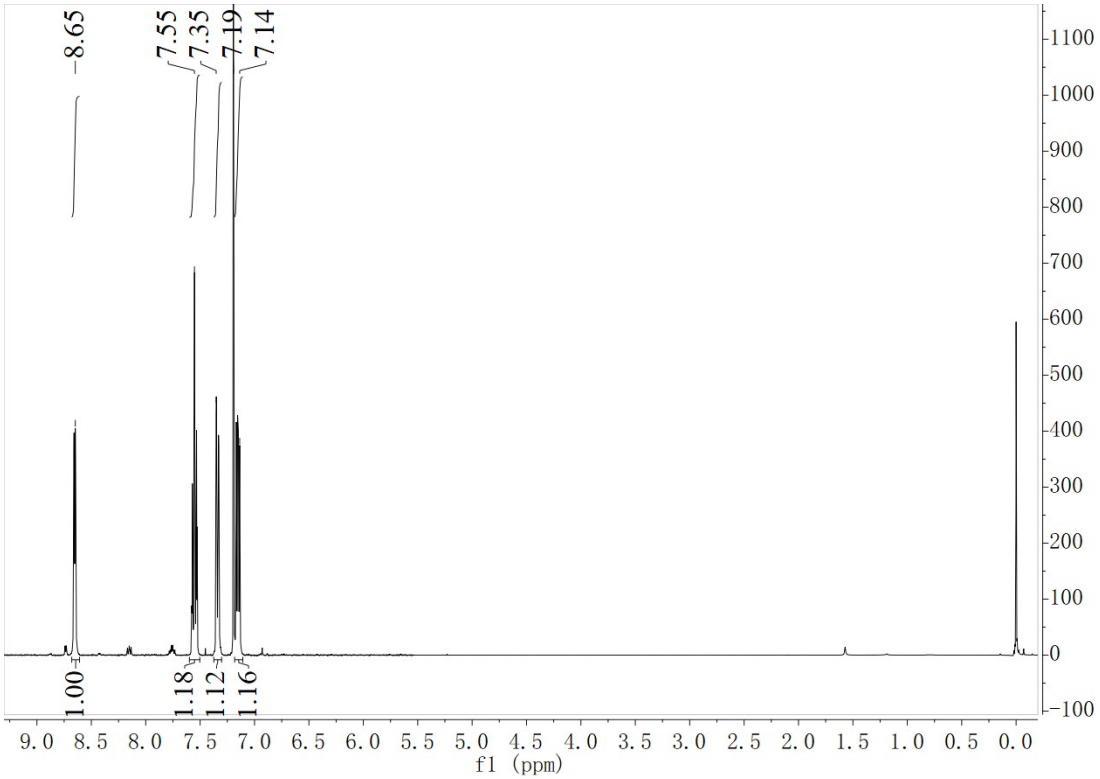

Fig. S1 The ^{1}H NMR spectrum of tri(2-pyridine)phosphine.

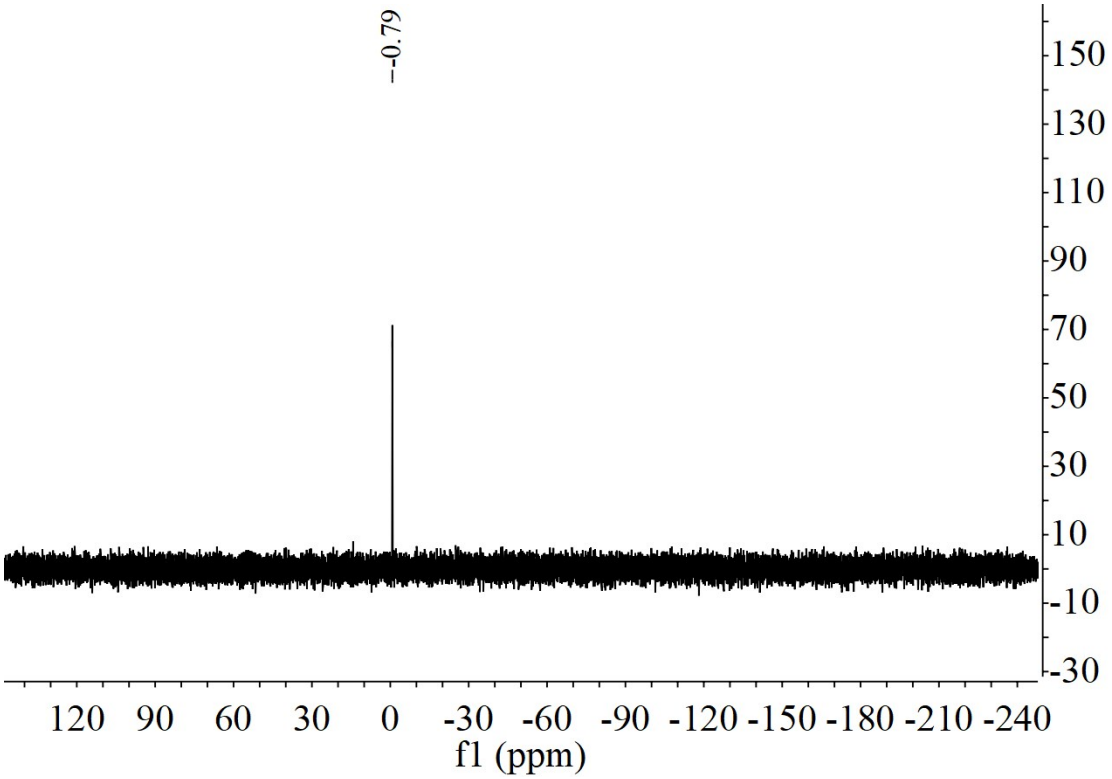

Fig. S2 The ^{31}P NMR spectrum of tri(2-pyridine)phosphine.

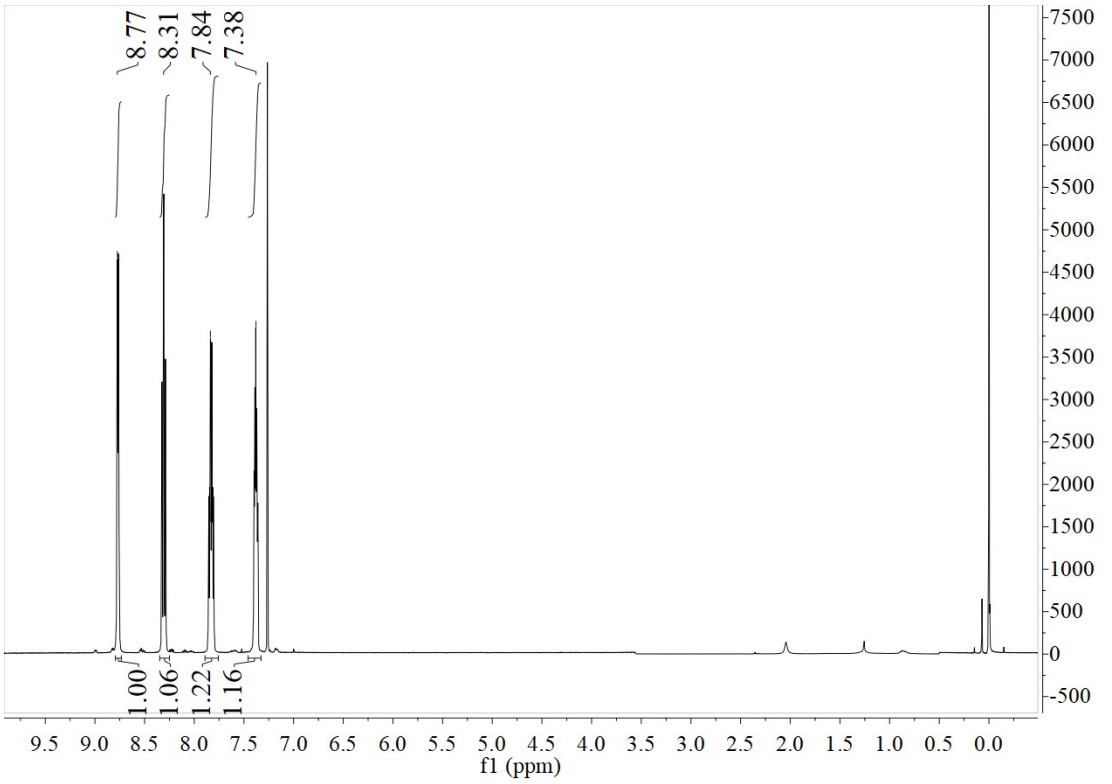

Fig. S3 The ^{1}H NMR spectrum of tri(pyridin-2-yl)phosphine sulfide.

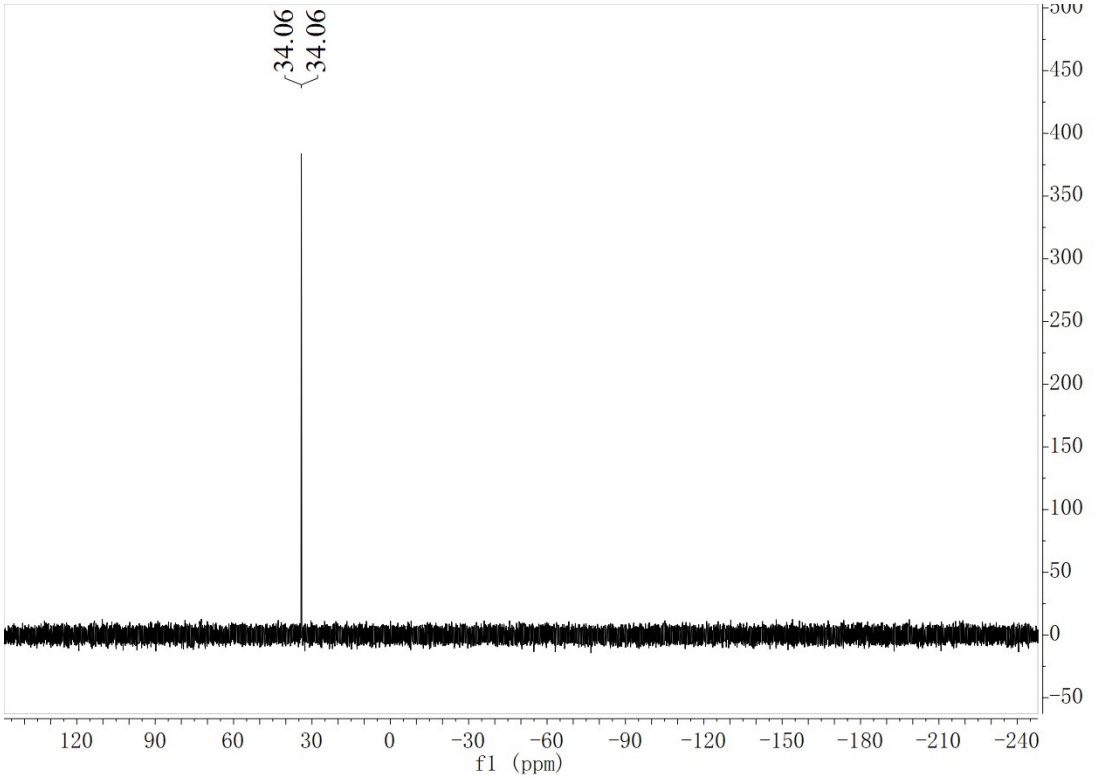

Fig. S4 The ^{31}P NMR spectrum of tri(pyridin-2-yl)phosphine sulfide.

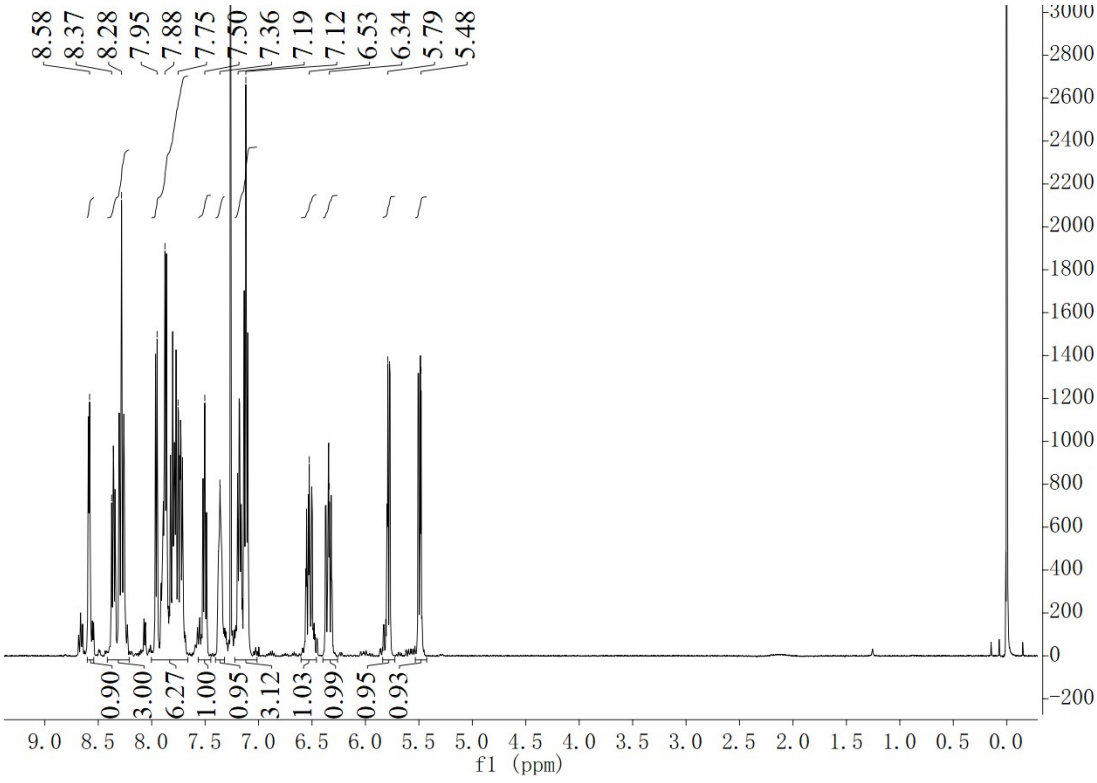

Fig. S5 The ^{1}H NMR spectrum of $Ir(dfppy)_2(sdpp)$.

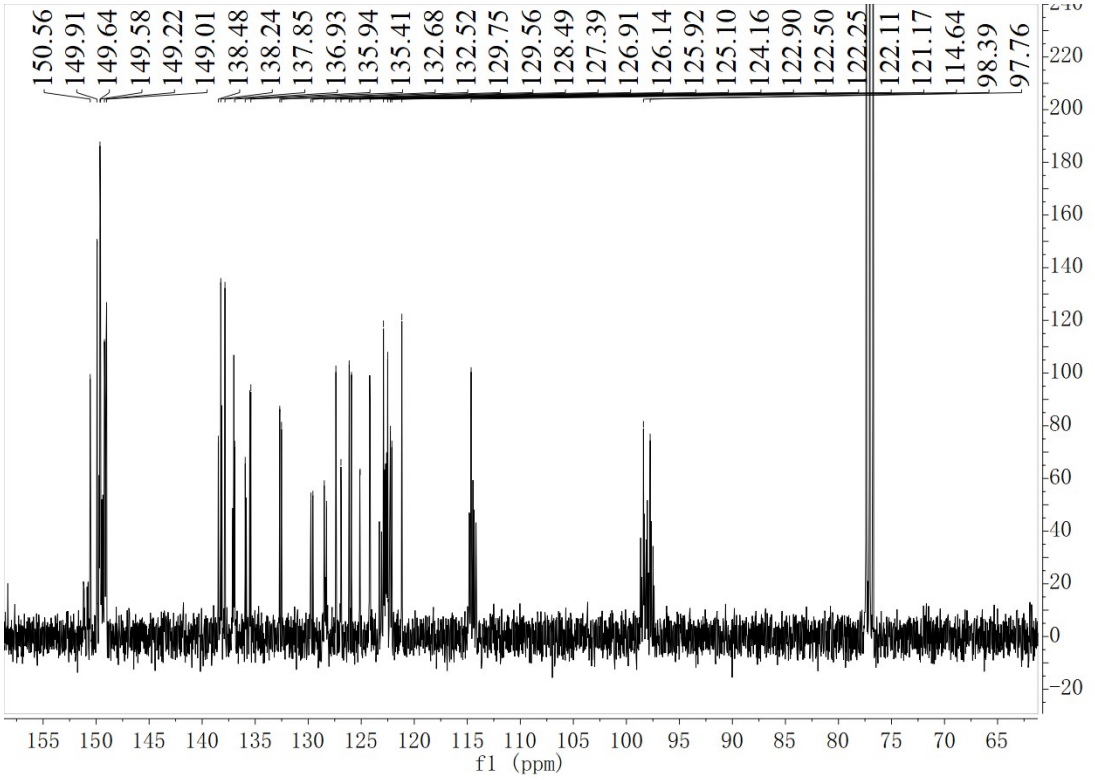

Fig. S6 The ^{13}C NMR spectrum of Ir(dfppy)$_2$(sdpp).

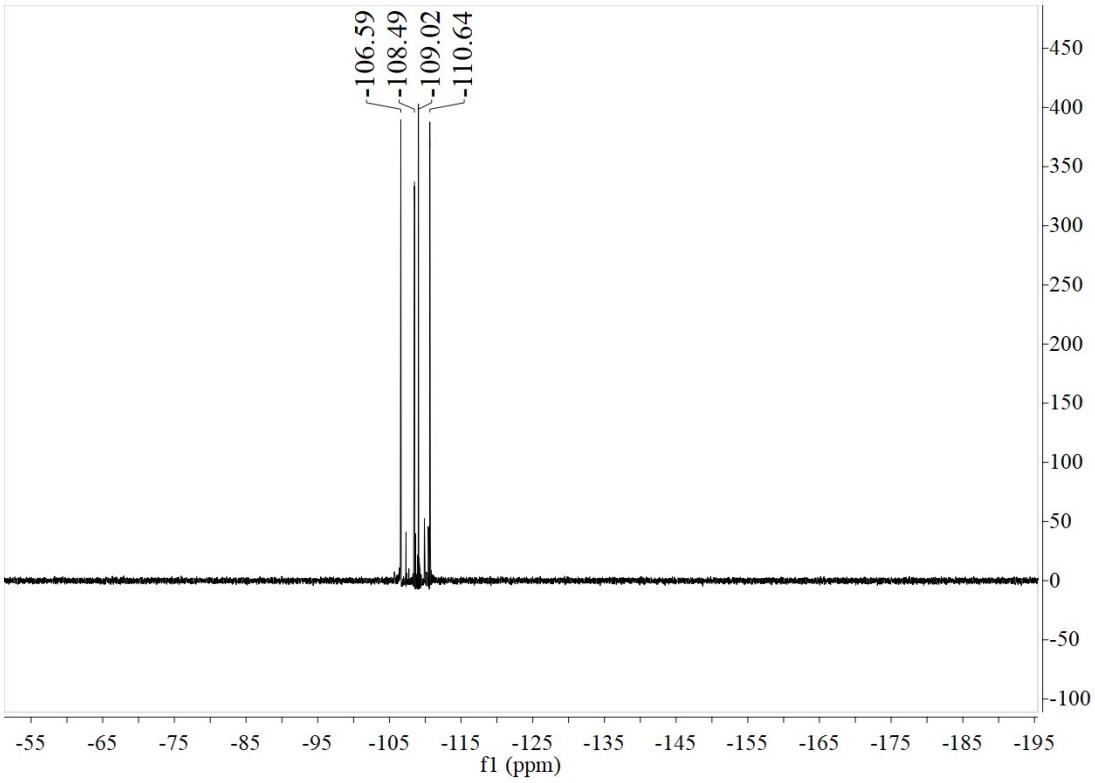

Fig. S7 The ^{13}F NMR spectrum of Ir(dfppy)$_2$(sdpp).

Fig. S8 The ^{13}P NMR spectrum of $Ir(dfppy)_2(sdpp)$.

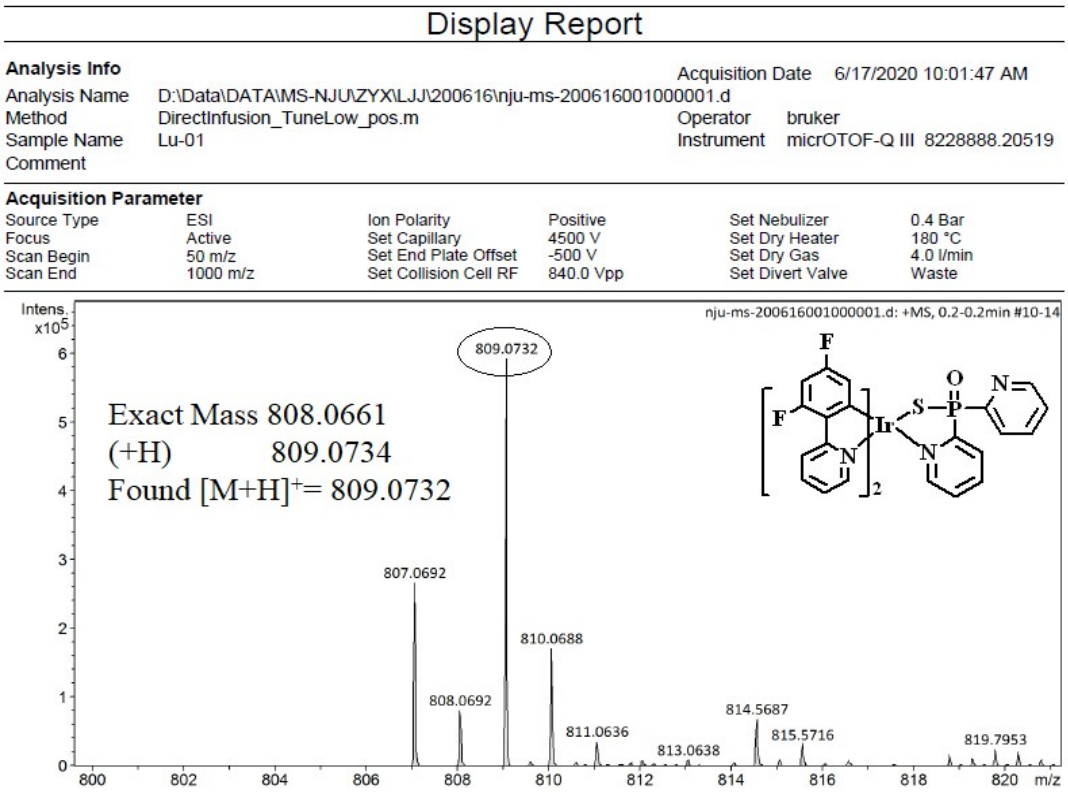

Fig. S9 The high-resolution MS spectrum of $Ir(dfppy)_2(sdpp)$.

2.4 X-ray crystallographic data

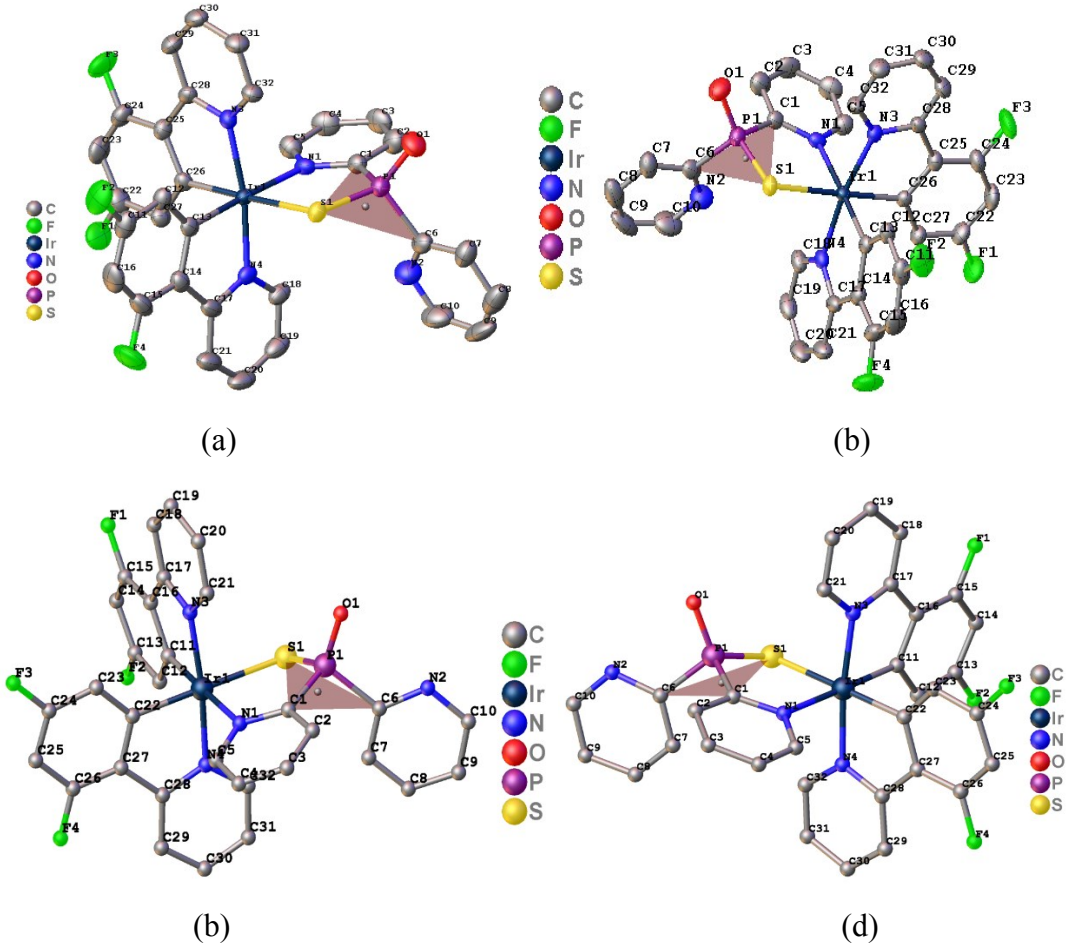

Fig. S10 Crystal structures of (a) λ-Ir(dfppy)$_2$(*S*-sdpp), (b) δ-Ir(dfppy)$_2$(*R*-sdpp), (c) λ-Ir(dfppy)$_2$(*R*-sdpp) and (d) δ-Ir(dfppy)$_2$(*S*-sdpp).

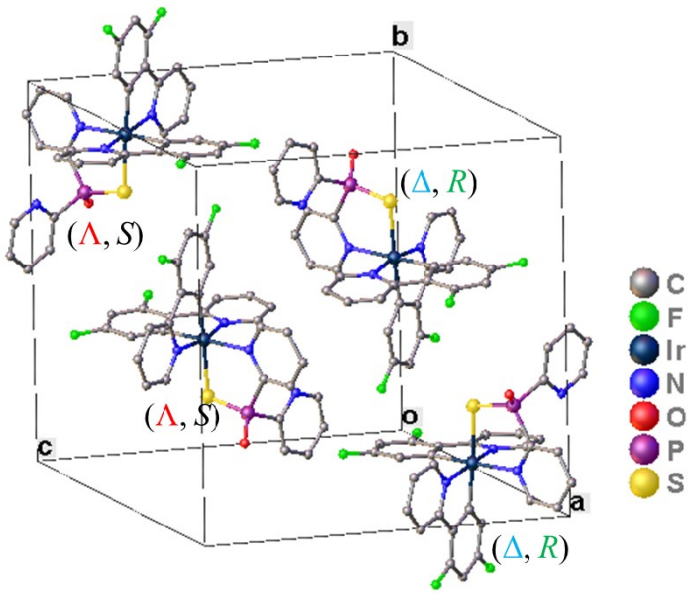

Fig. S11 Crystal structures of the enantiomers of λ-Ir(dfppy)$_2$(*S*-sdpp) and δ-Ir(dfppy)$_2$(*R*-sdpp) (CCDC: 2031307).

Table S1. Crystal data and structure refinement for the enantiomers of λ-Ir(dfppy)$_2$(*S*-sdpp) and δ-Ir(dfppy)$_2$(*R*-sdpp).

Dentification code	2031307
Empirical formula	$C_{32}H_{20}F_4IrN_4OPS$
Formula weight	807.75
Temperature/K	296(2)
Crystal system	monoclinic
Space group	$P2_1/n$
a/Å	12.887(3)
b/Å	16.441(3)
c/Å	15.163(3)
α/°	90
β/°	111.68(3)
γ/°	90
Volume/Å^3	2985.2(12)
Z	4
ρ_{calc}g/cm^3	1.797
μ/mm^{-1}	7.096
F(000)	1568.0
Crystal size/mm^3	0.15 × 0.12 × 0.09
Radiation	GaKα (λ = 1.34139)
2Θ range for data collection/°	7.188 to 108.01
Index ranges	-14 ≤ h ≤ 15, -19 ≤ k ≤ 18, -14 ≤ l ≤ 18
Reflections collected	18054
Independent reflections	5435 [R_{int} = 0.0323, R_{sigma} = 0.0313]
Data/restraints/parameters	5435/0/397
Goodness-of-fit on F^2	1.114
Final R indexes [I>=2σ (I)]	R_1 = 0.0276, wR_2 = 0.0689
Final R indexes [all data]	R_1 = 0.0300, wR_2 = 0.0701
Largest diff. peak/hole / e Å^{-3}	1.02/-0.79

Table S2. Bond Lengths for the enantiomers of λ-Ir(dfppy)$_2$(*S*-sdpp) and δ-Ir(dfppy)$_2$(*R*-sdpp).

Atom	Atom	Length/Å	Atom	Atom	Length/Å
Ir	S1	2.4714(11)	C5	C20	1.387(6)
Ir	N1	2.203(3)	C6	C8	1.467(5)
Ir	N2	2.040(3)	C6	C23	1.384(5)
Ir	N3	2.054(3)	C7	C24	1.376(6)
Ir	C1	2.009(4)	C8	C21	1.388(5)
Ir	C2	2.001(4)	C9	C26	1.377(6)
S1	P003	1.9963(15)	C10	C13	1.370(7)
P003	O1	1.496(3)	C10	C14	1.368(8)
P003	C7	1.831(4)	N4	C15	1.313(6)
P003	C15	1.815(4)	N4	C31	1.345(6)
N1	C7	1.358(5)	C11	C22	1.372(5)

N1	C9	1.324(5)	C12	C28	1.382(6)
N2	C5	1.378(6)	C13	F4	1.365(6)
N2	C12	1.342(5)	C15	C25	1.390(7)
N3	C8	1.360(5)	C16	C17	1.370(6)
N3	C16	1.348(5)	C17	C18	1.378(7)
F1	C22	1.357(5)	C18	C21	1.383(6)
F2	C14	1.360(5)	C19	C22	1.367(7)
C1	C0AA	1.406(6)	C19	C23	1.382(6)
C1	C4	1.397(6)	C20	C29	1.373(7)
F3	C23	1.369(5)	C24	C27	1.383(7)
C2	C6	1.414(5)	C25	C30	1.390(7)
C2	C11	1.398(5)	C26	C27	1.376(7)
C0AA	C5	1.451(6)	C28	C29	1.367(8)
C0AA	C13	1.388(6)	C30	C32	1.369(9)
C4	C14	1.365(6)	C31	C32	1.377(9)

Table S3. Bond Angles for the enantiomers of λ-Ir(dfppy)$_2$(*S*-sdpp) and δ-Ir(dfppy)$_2$(*R*-sdpp).

Atom	Atom	Atom	Angle/p	Atom	Atom	Atom	Angle/p
N(1)	Ir(1)	S(1)	87.20(8)	C(26)	C(25)	C(28)	115.1(3)
N(4)	Ir(1)	S(1)	89.82(8)	C(24)	C(25)	C(26)	118.4(4)
N(4)	Ir(1)	N(1)	97.79(13)	C(24)	C(25)	C(28)	126.5(4)
N(4)	Ir(1)	N(3)	170.77(12)	N(1)	C(1)	P(1)	121.2(3)
N(3)	Ir(1)	S(1)	97.38(9)	N(1)	C(1)	C(2)	121.6(4)
N(3)	Ir(1)	N(1)	88.37(12)	C(2)	C(1)	P(1)	117.0(3)
C(13)	Ir(1)	S(1)	92.24(10)	N(3)	C(28)	C(25)	113.4(3)
C(13)	Ir(1)	N(1)	177.97(13)	N(3)	C(28)	C(29)	120.2(4)
C(13)	Ir(1)	N(4)	80.26(15)	C(29)	C(28)	C(25)	126.4(4)
C(13)	Ir(1)	N(3)	93.64(14)	N(1)	C(5)	C(4)	123.3(4)
C(26)	Ir(1)	S(1)	176.98(10)	C(11)	C(16)	C(15)	116.8(4)
C(26)	Ir(1)	N(1)	94.26(13)	C(6)	N(2)	C(10)	116.9(5)
C(26)	Ir(1)	N(4)	92.60(13)	C(22)	C(27)	C(26)	120.0(4)
C(26)	Ir(1)	N(3)	80.04(13)	N(4)	C(18)	C(19)	122.1(5)
C(26)	Ir(1)	C(13)	86.39(14)	C(16)	C(15)	C(14)	123.6(5)
P(1)	S(1)	Ir(1)	101.94(5)	F(4)	C(15)	C(14)	119.8(5)
O(1)	P(1)	S(1)	117.50(14)	F(4)	C(15)	C(16)	116.5(4)
O(1)	P(1)	C(1)	109.7(2)	F(2)	C(11)	C(12)	118.7(5)
O(1)	P(1)	C(6)	108.7(2)	F(2)	C(11)	C(16)	118.0(4)
C(1)	P(1)	S(1)	107.75(13)	C(12)	C(11)	C(16)	123.3(5)
C(6)	P(1)	S(1)	108.79(15)	N(2)	C(6)	P(1)	117.0(3)
C(6)	P(1)	C(1)	103.48(19)	N(2)	C(6)	C(7)	124.1(4)
C(1)	N(1)	Ir(1)	121.9(3)	C(7)	C(6)	P(1)	118.8(3)
C(5)	N(1)	Ir(1)	120.1(3)	N(3)	C(32)	C(31)	122.6(4)
C(5)	N(1)	C(1)	117.9(4)	C(32)	C(31)	C(30)	118.9(4)
C(17)	N(4)	Ir(1)	116.2(3)	C(31)	C(30)	C(29)	119.1(4)
C(18)	N(4)	Ir(1)	124.1(3)	C(22)	C(23)	C(24)	116.3(4)

C(18)	N(4)	C(17)	119.6(4)	C(20)	C(21)	C(17)	120.0(5)
C(28)	N(3)	Ir(1)	116.4(2)	C(30)	C(29)	C(28)	120.1(4)
C(32)	N(3)	Ir(1)	124.3(3)	F(1)	C(22)	C(27)	118.3(4)
C(32)	N(3)	C(28)	119.1(3)	F(1)	C(22)	C(23)	118.3(4)
C(14)	C(13)	Ir(1)	114.2(3)	C(23)	C(22)	C(27)	123.3(4)
C(12)	C(13)	Ir(1)	126.1(3)	F(3)	C(24)	C(25)	120.3(4)
C(12)	C(13)	C(14)	119.7(4)	F(3)	C(24)	C(23)	116.0(4)
C(25)	C(26)	Ir(1)	115.0(3)	C(23)	C(24)	C(25)	123.7(4)
C(27)	C(26)	Ir(1)	126.7(3)	C(1)	C(2)	C(3)	119.9(4)
C(27)	C(26)	C(25)	118.3(4)	C(8)	C(7)	C(6)	117.9(5)
C(13)	C(14)	C(17)	116.3(4)	C(3)	C(4)	C(5)	119.2(4)
C(15)	C(14)	C(13)	117.4(4)	C(4)	C(3)	C(2)	118.0(4)
C(15)	C(14)	C(17)	126.3(4)	C(20)	C(19)	C(18)	118.6(5)
C(11)	C(12)	C(13)	119.1(4)	C(19)	C(20)	C(21)	120.3(4)
N(4)	C(17)	C(14)	112.9(3)	C(9)	C(8)	C(7)	118.7(5)
N(4)	C(17)	C(21)	119.4(4)	N(2)	C(10)	C(9)	123.4(5)
C(21)	C(17)	C(14)	127.7(4)	C(8)	C(9)	C(10)	118.9(5)

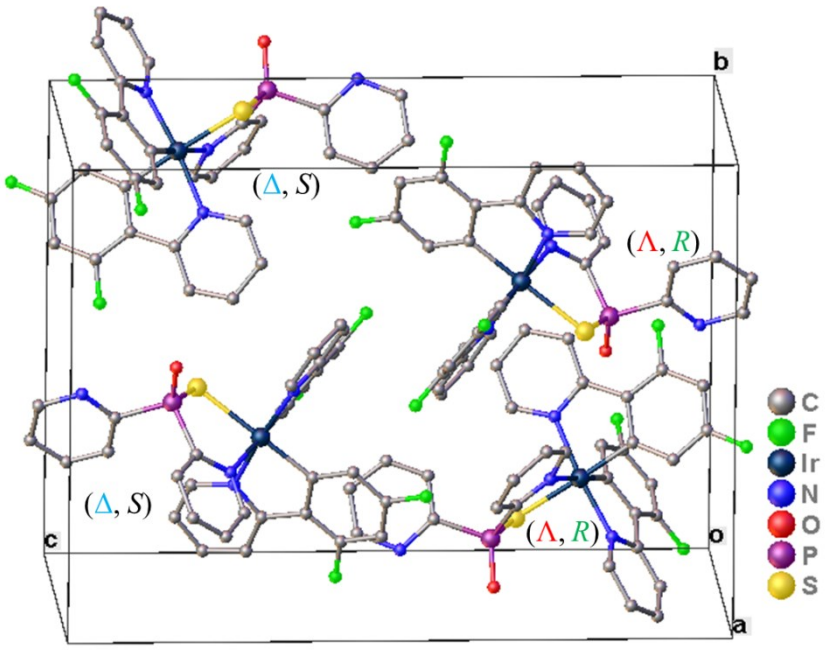

Fig. S12 Crystal structures of the enantiomers of δ-Ir(dfppy)$_2$(*S*-sdpp) and λ-Ir(dfppy)$_2$(*R*-sdpp) (CCDC: 1956514).

Table S4. Crystal data and structure refinement for the enantiomers of δ-Ir(dfppy)$_2$(*S*-sdpp) and λ-Ir(dfppy)$_2$(*R*-sdpp).

Identification code	1956514
Empirical formula	$C_{32}H_{21}F_4IrN_4OPS$
Formula weight	808.76
Temperature/K	296.15

Crystal system	monoclinic
Space group	$P2_1/n$
a/Å	9.1844(3)
b/Å	15.1203(4)
c/Å	20.3141(5)
α/°	90.00
β/°	91.0290(10)
γ/°	90.00
Volume/Å^3	2820.58(14)
Z	4
ρ_{calc}g/cm^3	1.905
μ/mm^{-1}	4.927
F(000)	1572.0
Radiation	MoKα (λ = 1.54780)
2Θ range for data collection/°	7.32 to 137.62
Index ranges	-9 ≤ h ≤ 11, -18 ≤ k ≤ 12, -20 ≤ l ≤ 24
Reflections collected	12831
Independent reflections	5004 [R_{int} = 0.0358, R_{sigma} = 0.0353]
Data/restraints/parameters	5004/1/382
Goodness-of-fit on F^2	1.110
Final R indexes [I>=2σ (I)]	R_1 = 0.0341, wR_2 = 0.0821
Final R indexes [all data]	R_1 = 0.0369, wR_2 = 0.0834
Largest diff. peak/hole / e Å^{-3}	1.20/-1.36

Table S5. Bond Lengths for the enantiomers of δ-Ir(dfppy)$_2$(*S*-sdpp) and λ-Ir(dfppy)$_2$(*R*-sdpp).

Atom	Atom	Length//Å	Atom	Atom	Length//Å
Ir(1)	S(1)	2.4655(14)	C(16)	C(15)	1.401(6)
Ir(1)	N(3)	2.042(4)	C(23)	C(24)	1.379(7)
Ir(1)	N(4)	2.038(4)	C(15)	C(14)	1.368(7)
Ir(1)	N(1)	2.170(4)	C(12)	C(13)	1.379(7)
Ir(1)	C(22)	2.016(5)	C(21)	C(20)	1.376(7)
Ir(1)	C(11)	1.992(5)	C(19)	C(20)	1.388(8)
S(1)	P(1)	1.9936(19)	C(19)	C(18)	1.385(8)
P(1)	O(1)	1.509(4)	C(24)	C(25)	1.373(8)
P(1)	C(1)	1.837(6)	C(27)	C(26)	1.382(7)
P(1)	C(6)	1.834(6)	C(27)	C(28)	1.462(7)
F(1)	C(15)	1.358(6)	C(32)	C(31)	1.384(7)
F(2)	C(13)	1.350(6)	C(5)	C(4)	1.392(7)
F(3)	C(24)	1.361(6)	C(26)	C(25)	1.386(8)
F(4)	C(26)	1.354(6)	C(1)	C(2)	1.384(7)
N(3)	C(17)	1.379(6)	C(7)	C(6)	1.343(8)
N(3)	C(21)	1.355(6)	C(7)	C(8)	1.351(9)
N(4)	C(32)	1.361(6)	C(4)	C(3)	1.371(9)
N(4)	C(28)	1.368(7)	C(28)	C(29)	1.410(7)
N(1)	C(5)	1.350(7)	C(3)	C(2)	1.403(9)

N(1)	C(1)	1.359(7)	C(14)	C(13)	1.386(7)
C(22)	C(23)	1.391(7)	C(30)	C(31)	1.392(9)
C(22)	C(27)	1.418(7)	C(30)	C(29)	1.388(9)
C(17)	C(16)	1.464(6)	C(6)	N(2)	1.384(8)
C(17)	C(18)	1.390(7)	N(2)	C(10)	1.411(10)
C(11)	C(16)	1.413(7)	C(8)	C(9)	1.393(12)
C(11)	C(12)	1.410(7)	C(10)	C(9)	1.396(11)

Table S6. Bond Angles for the enantiomers of δ-Ir(dfppy)$_2$(*S*-sdpp) and λ-Ir(dfppy)$_2$(*R*-sdpp)**.**

Atom	Atom	Atom	Angle/°	Atom	Atom	Atom	Angle/°
N(3)	Ir(1)	S(1)	87.59(11)	C(16)	C(15)	F(1)	120.5(4)
N(4)	Ir(1)	S(1)	97.30(12)	C(14)	C(15)	F(1)	115.7(4)
N(4)	Ir(1)	N(3)	173.43(15)	C(14)	C(15)	C(16)	123.8(5)
N(1)	Ir(1)	S(1)	88.01(12)	C(13)	C(12)	C(11)	118.9(4)
N(1)	Ir(1)	N(3)	99.10(15)	C(20)	C(21)	N(3)	122.7(5)
N(1)	Ir(1)	N(4)	85.50(15)	C(18)	C(19)	C(20)	118.7(5)
C(22)	Ir(1)	S(1)	175.88(13)	C(23)	C(24)	F(3)	118.6(5)
C(22)	Ir(1)	N(3)	94.45(17)	C(25)	C(24)	F(3)	117.4(5)
C(22)	Ir(1)	N(4)	80.40(18)	C(25)	C(24)	C(23)	124.1(5)
C(22)	Ir(1)	N(1)	95.19(17)	C(26)	C(27)	C(22)	118.3(5)
C(11)	Ir(1)	S(1)	91.32(13)	C(28)	C(27)	C(22)	115.5(4)
C(11)	Ir(1)	N(3)	80.37(17)	C(28)	C(27)	C(26)	126.1(5)
C(11)	Ir(1)	N(4)	95.08(17)	C(31)	C(32)	N(4)	121.8(5)
C(11)	Ir(1)	N(1)	179.17(17)	C(4)	C(5)	N(1)	122.1(5)
C(11)	Ir(1)	C(22)	85.49(18)	C(27)	C(26)	F(4)	120.5(5)
P(1)	S(1)	Ir(1)	99.52(7)	C(25)	C(26)	F(4)	116.5(5)
O(1)	P(1)	S(1)	116.58(19)	C(25)	C(26)	C(27)	123.0(5)
C(1)	P(1)	S(1)	107.53(17)	N(1)	C(1)	P(1)	120.7(4)
C(1)	P(1)	O(1)	112.1(2)	C(2)	C(1)	P(1)	118.0(4)
C(6)	P(1)	S(1)	106.35(19)	C(2)	C(1)	N(1)	121.3(5)
C(6)	P(1)	O(1)	111.7(3)	C(26)	C(25)	C(24)	116.4(5)
C(6)	P(1)	C(1)	101.3(3)	C(8)	C(7)	C(6)	117.2(6)
C(17)	N(3)	Ir(1)	116.4(3)	C(3)	C(4)	C(5)	119.4(6)
C(21)	N(3)	Ir(1)	125.0(3)	C(27)	C(28)	N(4)	113.4(4)
C(21)	N(3)	C(17)	118.6(4)	C(29)	C(28)	N(4)	120.0(5)
C(32)	N(4)	Ir(1)	123.8(4)	C(29)	C(28)	C(27)	126.5(5)
C(28)	N(4)	Ir(1)	116.4(3)	C(2)	C(3)	C(4)	118.8(5)
C(28)	N(4)	C(32)	119.8(4)	C(13)	C(14)	C(15)	116.1(4)
C(5)	N(1)	Ir(1)	120.4(3)	C(19)	C(20)	C(21)	119.3(5)
C(1)	N(1)	Ir(1)	120.7(3)	C(29)	C(30)	C(31)	119.3(5)
C(1)	N(1)	C(5)	118.8(4)	C(7)	C(6)	P(1)	116.1(4)
C(23)	C(22)	Ir(1)	126.3(4)	N(2)	C(6)	P(1)	118.9(5)
C(27)	C(22)	Ir(1)	113.9(4)	N(2)	C(6)	C(7)	124.9(6)
C(27)	C(22)	C(23)	119.8(4)	C(19)	C(18)	C(17)	120.6(5)

C(16)	C(17)	N(3)	112.4(4)	C(3)	C(2)	C(1)	119.5(5)
C(18)	C(17)	N(3)	120.1(4)	C(10)	N(2)	C(6)	116.9(7)
C(18)	C(17)	C(16)	127.4(4)	C(30)	C(31)	C(32)	119.3(5)
C(16)	C(11)	Ir(1)	114.9(3)	C(30)	C(29)	C(28)	119.7(6)
C(12)	C(11)	Ir(1)	126.3(4)	C(12)	C(13)	F(2)	118.7(5)
C(12)	C(11)	C(16)	118.8(4)	C(14)	C(13)	F(2)	117.2(4)
C(11)	C(16)	C(17)	115.6(4)	C(14)	C(13)	C(12)	124.0(5)
C(15)	C(16)	C(17)	125.8(4)	C(9)	C(8)	C(7)	123.1(8)
C(15)	C(16)	C(11)	118.5(4)	C(9)	C(10)	N(2)	119.6(7)
C(24)	C(23)	C(22)	118.4(5)	C(10)	C(9)	C(8)	118.3(7)

S3. HPLC Data

Chiral HPLC has been used in optical resolution of Ir(dfppy)$_2$(sdpp) to obtain the chiral Ir(III) complexes. HPLC Analysis Conditions: a) Column: Cat. No. EnantioPak®Y7, 5μm, 250 × 30 mm; b) Mobile phase: n-Hexane/Ethanol=80/20(v/v); c) Flow rate: 25.0 mL/min; d) Abs. detector: 254 nm.

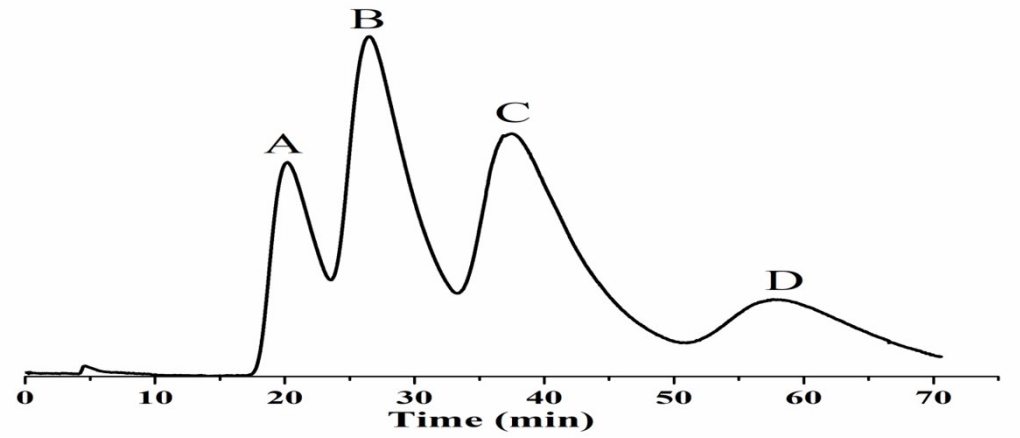

Fig. S13 HPLC profile of Ir(dfppy)$_2$(sdpp).

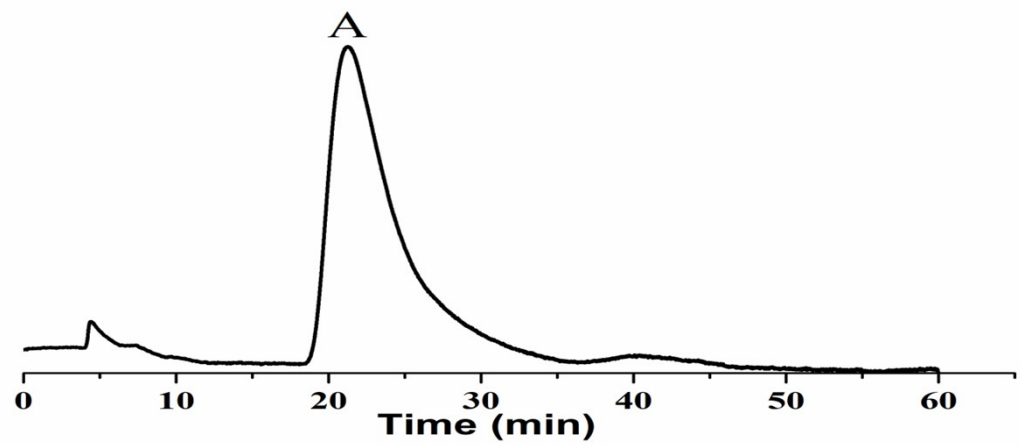

Fig. S14 HPLC profile of δ-Ir(dfppy)$_2$(*R*-sdpp).

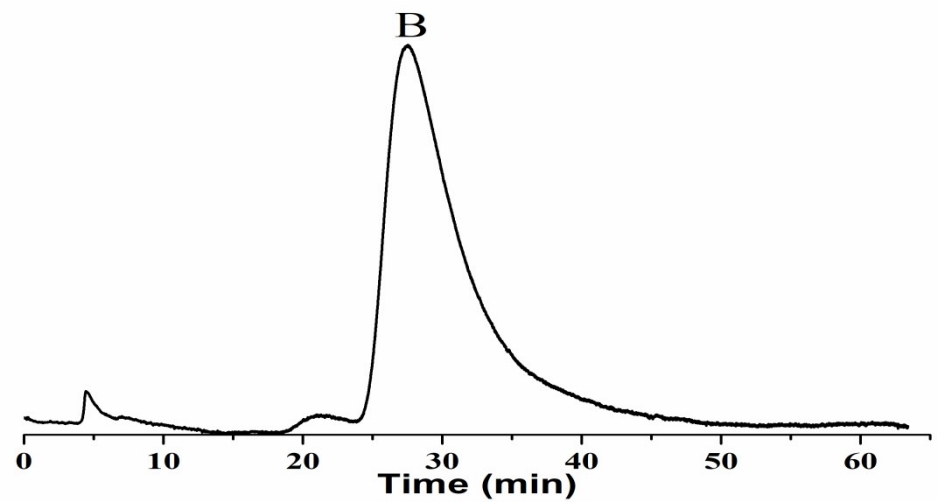

Fig. S15 HPLC profile of λ-Ir(dfppy)$_2$(*R*-sdpp).

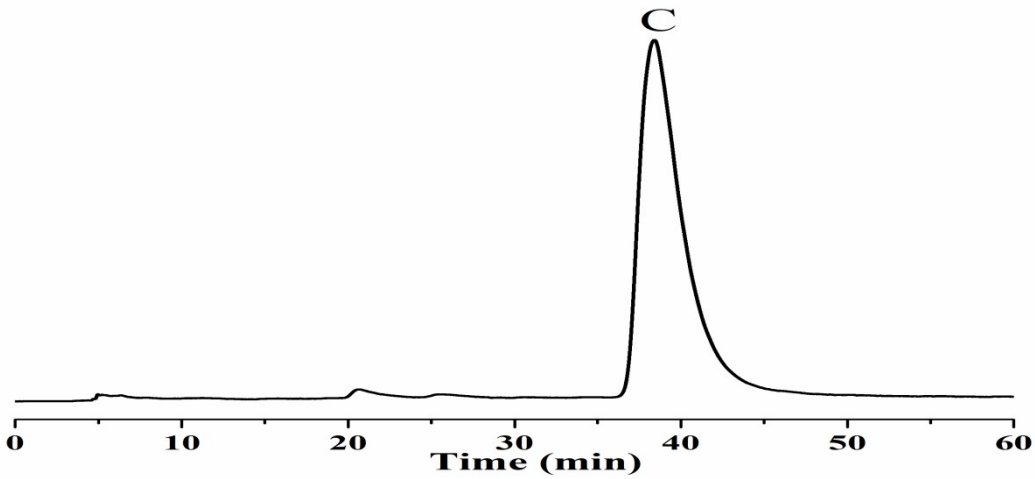

Fig. S16 HPLC profile of λ-Ir(dfppy)$_2$(*S*-sdpp).

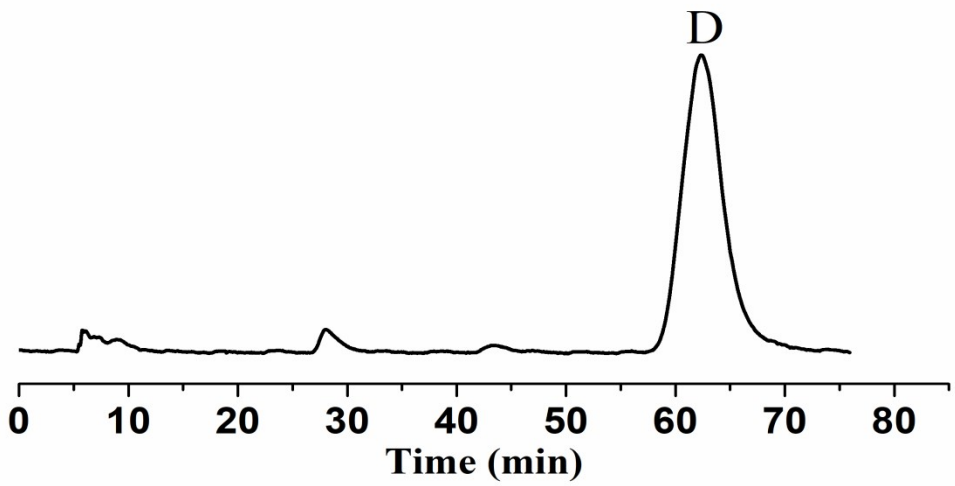

Fig. S17 HPLC profile of δ-Ir(dfppy)$_2$(*S*-sdpp).

S4. Photophysical and chiral optical measurement

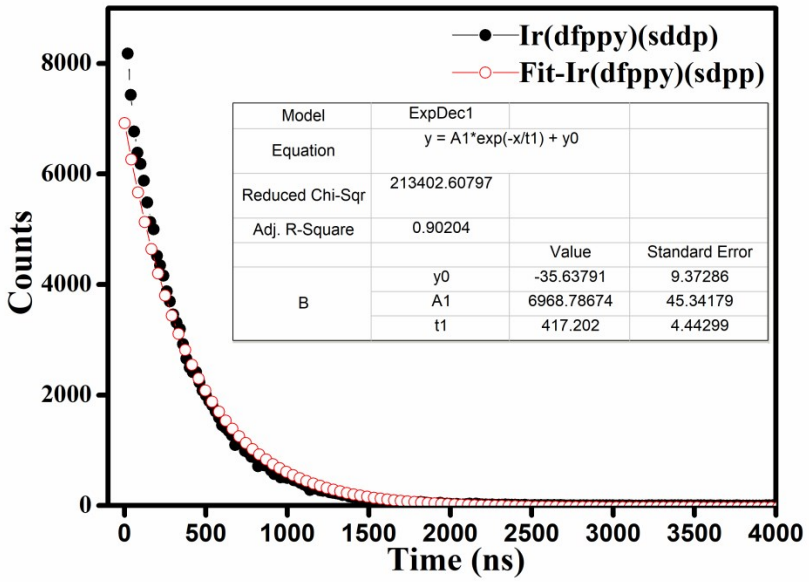

Fig. S18 The lifetime curve of $Ir(dfppy)_2(sdpp)$ in degassed CH_2Cl_2 solution at room temperature.

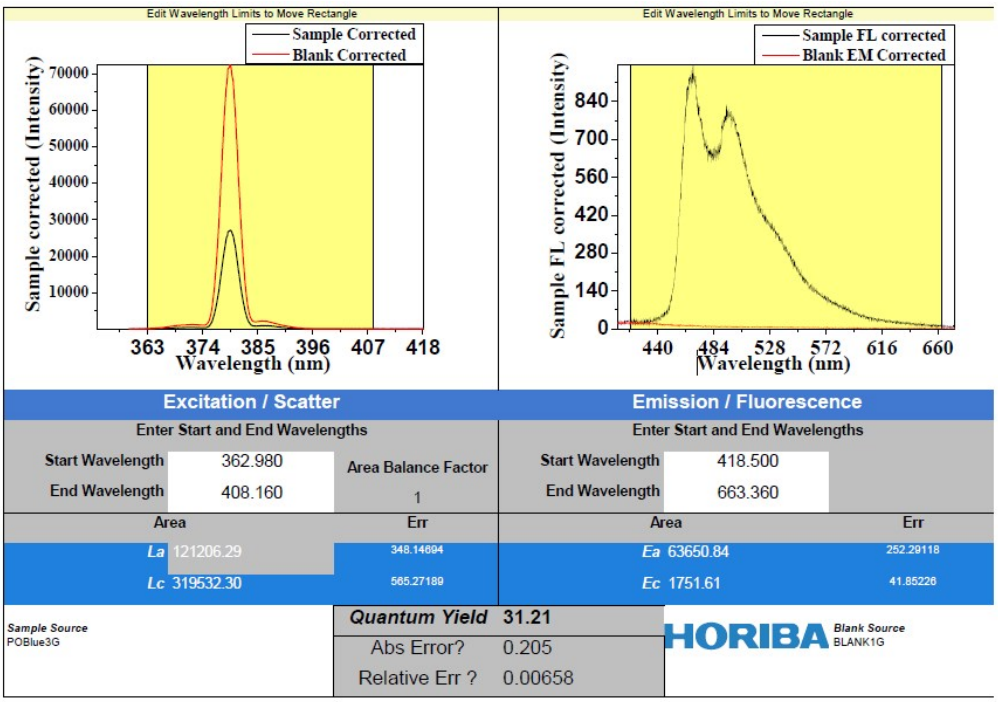

Fig. S19 The quantum yield measurement of $Ir(dfppy)_2(sdpp)$ in degassed CH_2Cl_2 solution at room temperature.

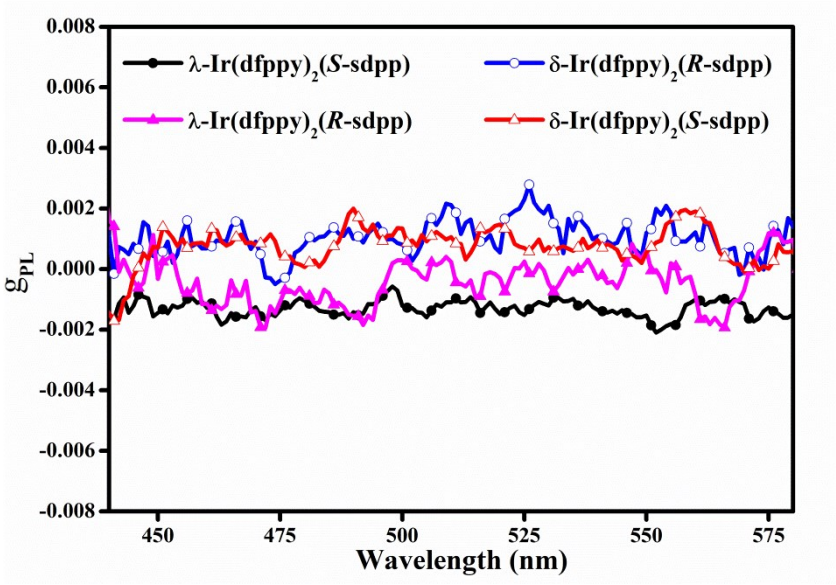

Fig. S20 g_{PL} values of λ-Ir(dfppy)$_2$(*S*-sdpp) and δ-Ir(dfppy)$_2$(*R*-sdpp), λ-Ir(dfppy)$_2$(*R*-sdpp) and δ-Ir(dfppy)$_2$(*S*-sdpp) in degassed CH_2Cl_2 solution.

S5. Electrochemical measurement

Cyclic-voltammetry measurement system was performed at room temperature in deaerated CH_2Cl_2, employing a polished Pt plate as the working electrode, and tetra-*n*-butylammonium perchlorate (0.1M) as the supporting electrolyte, Fc^+/Fc was used as the reference, with the scan rate of 0.1 V/s. The energy levels were calculated using the following equations: HOMO = -(4.8 + E_{ox}) eV, LUMO = HOMO + E_g, E_g was calculated from the UV-vis absorption spectrum.

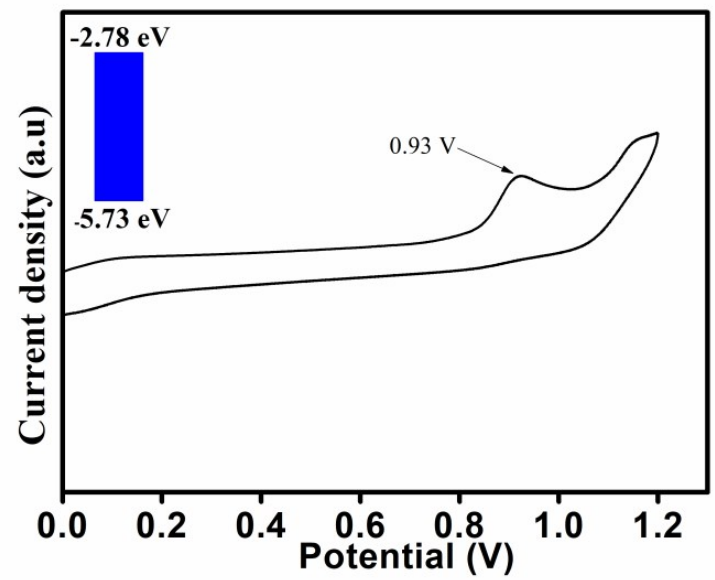

Fig. S21 The cyclic voltammogram curve of Ir(dfppy)$_2$(sdpp).

S6. Theoretical calculation

Table S7. The calculated energy levels and spatial distributions of HOMO and LUMO of λ-Ir(dfppy)$_2$(*S*-sdpp) and δ-Ir(dfppy)$_2$(*R*-sdpp), λ-Ir(dfppy)$_2$(*R*-sdpp) and δ-Ir(dfppy)$_2$(*S*-sdpp).

Complexes	Orbital	Composition (%)		
		Ir	Main ligand	Ancillary ligand
λ-Ir(dfppy)$_2$(*S*-sdpp)	HOMO	43.78	34.90	21.32
	LUMO	6.04	83.16	10.80
δ-Ir(dfppy)$_2$(*R*-sdpp)	HOMO	43.80	33.98	22.22
	LUMO	6.04	83.02	10.94
λ-Ir(dfppy)$_2$(*R*-sdpp)	HOMO	42.19	30.45	27.36
	LUMO	4.78	82.43	12.79
δ-Ir(dfppy)$_2$(*S*-sdpp)	HOMO	42.18	30.56	27.26
	LUMO	4.78	86.65	8.57

S7. Thermal stability

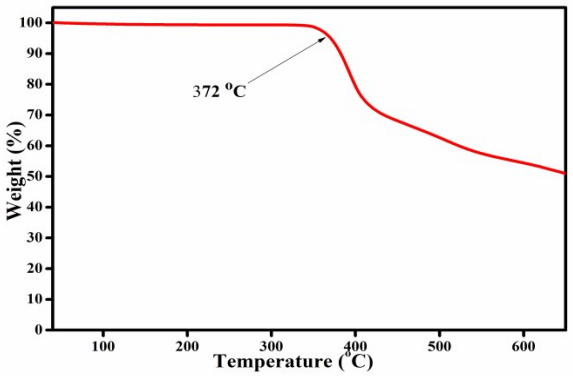

Fig. S22 The TGA curve of Ir(dfppy)$_2$(sdpp).

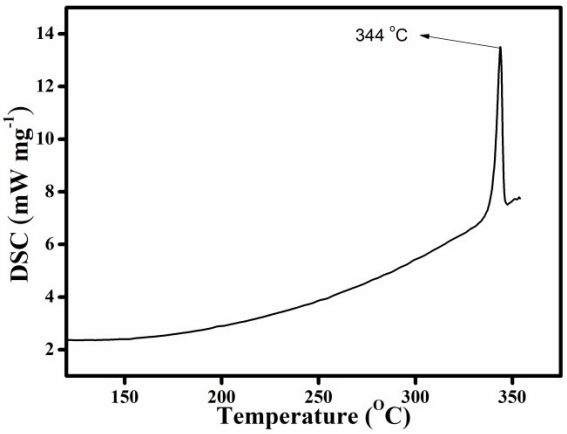

Fig. S23 The DSC curve of Ir(dfppy)$_2$(sdpp).

S8. Device fabrication and characterization

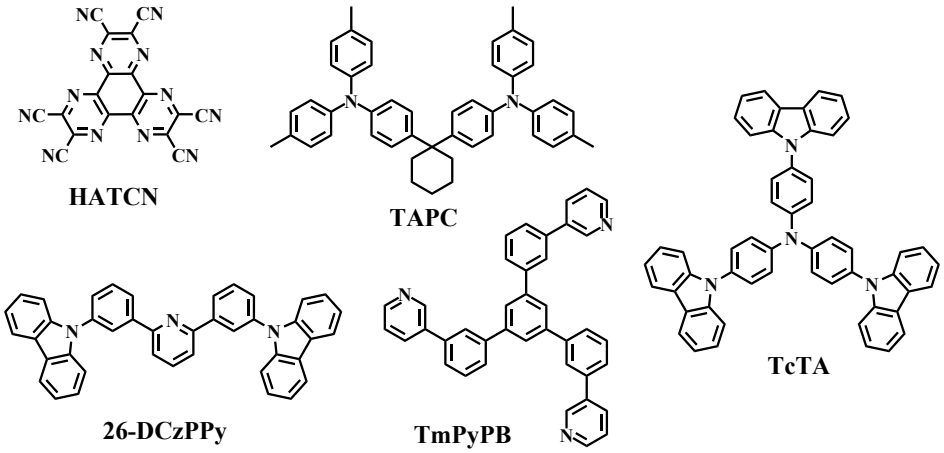

Fig. S24 The molecular structures of the compounds used in the device.

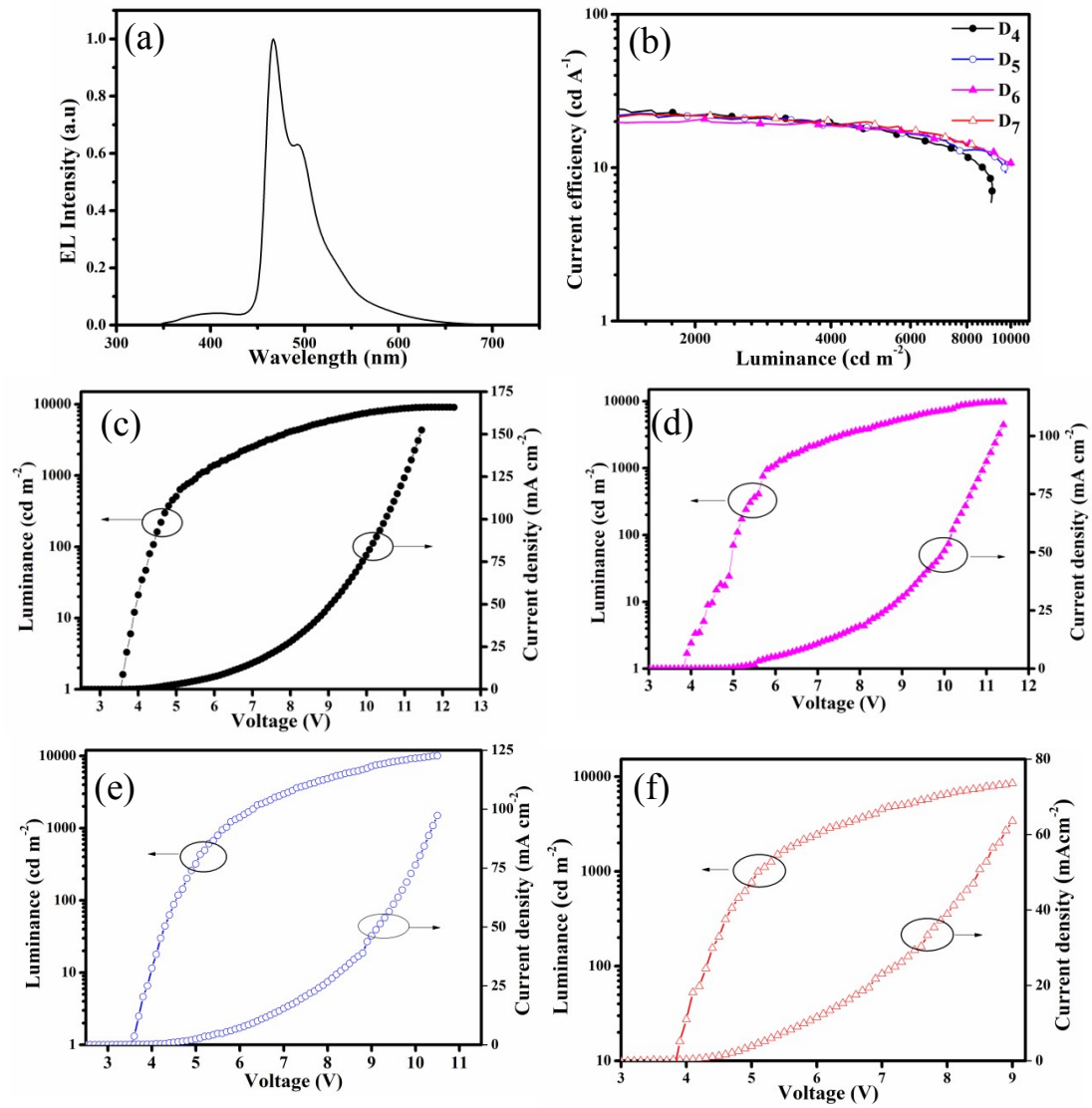

Fig. S25 (a) EL spectrum (6 V) of CP-OLEDs, (b) Current efficiency-Luminance curves, Luminance-voltage-current density performance of CP-OLEDs based on (c) λ-Ir(dfppy)$_2$(*S*-sdpp) and δ-Ir(dfppy)$_2$(*R*-sdpp), λ-Ir(dfppy)$_2$(*R*-sdpp) and δ-Ir(dfppy)$_2$(*S*-sdpp).

S9. Reference

1. SAINT-Plus, version 6.02, Bruker Analytical X-ray System, Madison, WI, 1999.
2. G. M. Sheldrick, SADABS An empirical absorption correction program, Bruker Analytical X-ray Systems, Madison, WI, 1996.
3. G. M. Sheldrick, SHELXTL-2014, Universität of Göttingen, Göttingen, Germany, 2014.
4. O. V. Dolomanov, L. J. Bourhis, R. J. Gildea, J. A. K. Howard and H. Puschmann, "OLEX2: a complete structure solution, refinement and analysis program". *J. Appl. Cryst*., 2009, 42, 339-341.